Bulk Phase Water Diffusion is Significantly Inhibited by Inhomogeneity of Single Non-crystal Particle at Low Relative Humidity

Chen Cai,[1] Stephen Ingram[2] and Chunsheng Zhao[1]*

[1]*Department of Atmospheric and Oceanic Sciences, School of Physics, Peking University, Beijing 100871, China*

[2]*School of Chemistry, University of Bristol, Cantock's close, Bristol BS8 1TS, UK*

Corresponding author: Chunsheng Zhao (86-10-62754684, zcs@pku.edu.cn)

Abstract

It has been suggested by recent studies that atmospheric particles adopt non-crystalline states which significantly impact aerosol-cloud interactions and atmospheric chemistry. In this study, the effect of different, non-crystalline states on water diffusion is investigated in detail, from single multi-component particles, levitated in aerosol optical tweezers. We infer the time-dependent particle size from Raman spectra using Mie fitting, and thus derive the translational diffusion coefficient of water (D_{water}) from particle radius changes during evaporation or condensation processes. Both glassy states (in saccharide particles) and gel states (in magnesium sulfate) are investigated. In both cases the bulk phase water diffusion is shown to be severely restricted, thus limiting the gas-particle water partitioning on the particle surface. The D_{water} of non-crystalline particles generally gradually decreases as the concentration of the solute in the particle increases, while the relative humidity (RH) - D_{water} relationship of particle in gel state is complicated and brings huge deviation of D_{water} determination. We therefore present the time dependent water content at different location (radial coordinate) of the particle. The time scale required for particle to get equilibrium to environmental RH is vastly extended by the kinetic inhibition of bulk phase water transfer. This can give direct and quantitative indication of water diffusion within single non-crystal particle and its effect on gas-particle partitioning and equilibrium.

Keywords

Atmospheric particle; optical levitation measurement; non-crystalline; water transfer inhibition; bulk phase inhomogeneity

1. Introduction

Atmospheric particles with certain components might exist in non-crystalline state under certain range of relative humidity (RH) and temperature. The existing states might include ultra-viscous liquids, glasses, gels and etc.[1,2] Once the non-crystalline state is formed in the particle bulk phase, the particle will persist dis-equilibrium with surrounding environment for quite a long time.[3,4] This is usually accompanied with a much higher bulk phase viscosity (often more than 10 orders of magnitudes higher). In water evaporation process, water on the near-surface of a particle will rapidly evaporate into the surrounding gas phase. This is usually faster than the water transport from the interior of particle to the surface driven by bulk phase composition readjustment. Therefore, the less volatile solute will enrich at the gas-particle interface and inhibit interface water transport.[5-7] In water condensation process conversely, water condensed on the non-crystalline particle would form a infinite thin liquid shell, thus leads to the dissolution of interior part of particle.[5,8] The dissolution process of particle is composed of several transient inhomogeneous states.[5,8] As non-crystalline state is quite different from aqueous state, particle exist in non-crystalline state would presents various unique properties and effects. Non-crystalline particles can act as heterogeneous ice nuclei (IN) and play an important role in cirrus cloud formation. As the bulk phase diffusion is much slower, it would severely influence the timescale of cloud droplet formation.[9,10] Solute in non-crystalline particles usually exist in super-saturated state, and this would lead to forming of fewer and larger ice crystals with higher sedimentation velocity. This is particularly crucial in tropical tropopause, as the water would transport to the stratosphere from extremely cold and dry condition.[9] It is also suggested in previous studies that water transport in particles with high viscosity is still relatively rapid in comparison to other atmospheric process except when the particle is under extreme dry and cold condition.[2,8-11] Lower bulk phase diffusion may limit particle growth, make the equilibration times hugely larger than typical atmospheric residence time, and potentially leads to incorrect estimation

on gas-particle partitioning of low volatility component.[12,13] The disequilibrium between the composition of particle and surrounding condition[14-16] can also contribute to erroneous evaluation of particle and environmental composition.[17] Limited particle bulk phase diffusion can also affect its chemical reactivity, thus increasing the chemical lifetime of condensed organics significantly.[18-21] By prolonging the gas-particle interactions, the low diffusion rate would further impact the particle optical properties.[6,12,13]

Based on all the knowledge stated above, we need a quantitative estimation of D_{water}, in order to accurately and reliably investigate gas-particle partitioning. When RH decreases to a low enough value, organic aerosol will gradually and reversibly transit to an ultra-viscous glassy state, where its viscosity experiences exponential increase towards decreasing RH. In a glassy particle, water often acts as the plasticizer as it is usually the most mobile component.[2,22] In previous studies, the properties of glassy particle and its similarities and differences to crystalline particle have been preliminarily investigated.[1] It is also noted the glassy state can be formed in secondary organic aerosol (SOA) under ambient atmospheric conditions.[23] In Zobrist et al.'s study,[6] the framework for D_{water} determination from water uptake on electronic or optical levitated aqueous sucrose particle have been utilized. Determination of D_{water} in glassy particles is difficult as the diffusion is non-linear resulting from the plasticizing effect of water.[6,7,13] In various reported works, D_{water} is derived from the bulk phase viscosity which is easier to be measured. The viscosity of SOA or its proxies have been measured in various works.[5,23,24] The Stokes-Einstein equation has been adopted for D_{water} estimation from bulk phase viscosity of glassy state. However, this method is usually not available as it is hydrodynamic and not applicable for non-liquid state, especially when the mobility of water largely deviates from the mobility of solute molecule.[25-27] Therefore, direct measurement of diffusion is severely required as it would definitely provide direct and precise results than inference from viscosity.

While the diffusion and morphology of glassy aerosol have been widely investigated,[28-30] few

results of gel state particle diffusion have been reported. Different from the glassy particle, the gel state is a two-phase mixture in which liquid is dispersed in an amorphous matrix composed of colloidal or polymer network. It has been reported the porous gel state is formed in the dehydration of some organic particles.[1] It is noted in previous measurements of bulk diffusional kinetics that the formation of gel state would limit molecular diffusion near the gas-particle interface thus kinetically limit water absorption of particle.[33-35] Hydration would conversely discretely change the particle water content and gradually swell the particle. Structural defects in particle bulk phase would accelerate water uptake and reduce time of particle transition to fully solubilized state at deliquescence.[31-32] For most gel-forming particles, the initial gel state swelling would occurs with an increasing RH at a RH of around 30–40% and the whole deliquescence process might occur over a much broader RH range of 30-90%, depending on the solute solubility.[1]

The magnesium sulfate ($MgSO_4$) particle has received significant attention among various species of gel forming particles due to its prevalence in the sea spray aerosol.[10,36,37] In highly supersaturated $MgSO_4$ particle (with a solvent solute molar ratio larger than 6), the presence of contact ions polymeric structure would contributes to gel formation and may further limit water transport.[10,36] Buchner et al.[38] have detailed the specifics of the $MgSO_4$ ion pairing structure. Many bonding structures Buchner et al.[38] have detailed the specifics of the $MgSO_4$ ion pairing structure. Many bonding structures Buchner et al.[38] have detailed the specifics of the $MgSO_4$ ion pairing structure. Many bonding structures are adopted, for instance free hydrated ions, solvent-shared ion pairs and contact ion pairs, and would vary and transform to the changes in RH and solute concentration. $MgSO_4$ aqueous particles have also been deposited on the hydrophilic substrate and measured with confocal Raman spectroscopy to investigate their spatial structure and compositional distribution.[10,37] The inhibition of water transport and delaying of chain-structured contact ion pairs decomposition of $MgSO_4$ aqueous

particle during RH increasing is observed at the RH of ~40%. Li et al.[39] examined the isotope exchange between the $MgSO_4$ - D_2O particle and ambient H_2O water vapor. The kinetics water exchange between $MgSO_4$ particles and surrounding environment is spatially observed. The composition at the particle center and surface were acquired from confocal Raman spectra and compared, indicating the presence of significant bulk phase in-homogeneity within the particle.

In this study we evaluated the formation of both non-crystalline glassy and gel states within levitated single particles and their influence on restricting bulk phase water transfer. We acquired the time dependent size from Mie fits to collect Raman spectra and investigated the water diffusion corresponding to step changes in RHs. In section 2, details of the optical levitation experiments conducted in this study are introduced. In section 3, results of water transport kinetics and compositional inhomogeneity of glass particle and gel particle are illustrated. By presenting the RH-D_{water} correlations, we illustrate the bulk phase water transport inhibition from inhomogeneity of particle bulk phase, and its direct effect on water partitioning and in-equilibrium between the particle and surrounding gas phase. Additionally, we investigated time-dependent composition at different positions of the levitated particle, indicating the required timescale for non-crystal particles to reach equilibrium with the surrounding environment. This study provides direct and quantitative indication of retarded water diffusion within a single particle and its influences on gas-particle partitioning and equilibrium.

2. Experimental Descriptions

Details of the mechanism and setup of aerosol optical tweezers have been described in previous studies and will only be briefly mentioned here.[40] A 532 nm laser beam (Gaussian distributed cross section intensity, initial power ~200 mW, trapping power ~20-50 mW) generated from a semiconductor laser (Laser Quantum, Opus-6000 532 nm) is adopted as the trapping and stimulating laser. The laser pass through the coverslip of the sample chamber after being focused through an immersion objective

(Olympus UIS2 PlanCN, 100×, 1.25 N.A., glycerol as transmitter) to form the single trapping position. Particles are nebulized from a medical nebulizer (Yuyue 402AI model) and then injected into the sample chamber. The nebulized particles would pass through the focus, and is then pulled into the focal point of the laser by the gradient force from the focused beam. The trapped particle can then collide and coalesce with other particles flowing in the sample chamber and grow larger.

The stimulated cavity enhanced Raman signal of the trapped particle is focused and directed into a spectrograph (Zolix Omnic λ-300i), then spatially resolved through a 1200 groves mm^{-1} grating and acquired by the CCD (Andor Solis 256, pixel array 1024×256). The accumulating time of single spectra is usually 0.5 or 1 s. The size and real part of refractive index of levitated particle is calculated from the Mie fit of stimulated Raman fingerprint in the wavelength range of 630 - 660 nm. Light from a 455 nm LED is introduced as illumination light, irradiate the particle and propagate into a CCD (Watec, 1/3 in., model 231S2) which records the bright-field images.

A dry and a wet N_2 gas flow are merged and introduced into the chamber through a pair of mass flow controllers (D_{mass}, DFC10-1/4-N_2-3000SCCM-B01). RH and temperature in the chamber can be controlled by adjusting the ratio of dry and wet N_2 gas flows. The combined gas flow introduced into the chamber was maintained constant at 250 sccm. Two RH-T detectors (Vaisala Humidity and Temperature Meter Series HMT330) positioned at the entrance and exit of the chamber. Time dependent RH and temperature in the chamber can thus be recorded. All solutions for particle preparation were prepared by dissolving analytical grade solute (Shanghai Chemistry) in triple distilled water.

3. Results and Discussion

In this study, we demonstrate the existence of inhibitions to bulk phase water transport in both glassy state particle (sucrose/glucose ternary aqueous particle) and gel state particle ($MgSO_4$ aqueous particle), and detail the differences in the limiting D_{water} value with reference to the current literature view of the molecular structure.

3.1. Water transport kinetics in sucrose-glucose aqueous (glassy state) particle

For the investigation of water transport kinetics of glassy state, we present results of sucrose/glucose aqueous particle in this study. As the diffusion of sucrose and glucose particle present different degrees of water transport limitation, results of sucrose/glucose aqueous particle with different composition ratio of sucrose and glucose can provide relevance between bulk phase diffusion, composition distribution and equilibrium time scale. Time-dependent RH and corresponding particle radius of sucrose/glucose aqueous particle from a typical RH varying experiment are shown in Figure 1. As the RH decrease below ~40%, time required for radius response towards RH changes is much larger. In the two time-dependent size steps between ~42 000 s and ~58 000 s, although the RH changes from ~81% to ~25% and then return to the initial level, the particle radius cannot return to the initial level of ~5025 nm at ~42 000 s, as there is obvious kinetic effects on bulk phase water transport and particle radius changes.

In order to give quantitative assessment of kinetic water transport limitation within sucrose-glucose aqueous particle at lower RH, we investigate the timescale of water transport in the levitated particle by calculating the characteristic relaxation time of particle size, τ, as τ is a reliable indicator of water transport rate directly measured from particle size variation.[41,42] Since the diffusion rates at different radial coordinate of the particle bulk phase might vary over several orders of magnitude, timescale of relaxation at different position in the particle might synchronously ranges across a wide range

of magnitude, made the simple exponential function not adoptable for accurate description of the size changes of non-crystalline particle. As stretched exponential relaxation behavior is common on various properties of non-crystalline, if we use a simple exponential expression to fit the size relaxation step, τ might be quite far from the true one. Therefore, we adopt the Kohlrausch-Williams-Watts (KWW) equation to precisely fit individual size relaxation step in this study.[42,43] In KWW equation, the time-dependent particle size is expressed as,[3]

$$r(t) \approx r(\infty) + \big(r(0) - r(\infty)\big)\exp\left[-\left(\frac{t}{\tau}\right)^{\beta}\right] \qquad (1),$$

in which τ presents the characteristic time constant and β is stretch parameter of the size relaxation. Currently the chemical significance of β still remains unclear. As noted in previous studies,[44,45] β represents particle heterogeneity. Although relaxation of individual molecule through the particle is exponential, the dynamic evolution of particle is intrinsically non-exponential.[46] Therefore, the KWW fit can give direct and precise analysis of particle evolution kinetics through presenting the fractional progression of particle size relaxation between initial and final states.

The fitted characteristic time τ and stretch parameter β of particle radius relaxation with three sucrose/glucose mass ratios are shown in Figure 2(a-b, mf(Sucrose):mf(Glucose) = 3:1), (c-d, mf(Sucrose):mf(Glucose) = 1:1), and (e-f, mf(Sucrose):mf(Glucose) = 1:3). There are 130, 166 and 111 transitions of particles with sucrose/glucose mass ratios of 3:1, 1:1, 1:3 between various initial and final RHs being KWW fitted. Plots on the right-down side of the diagonal correspond to RH decreasing steps (particle evaporation) while plots on the left-up correspond to RH increasing steps (particle condensation). The fitted τ in Figure 2(a, c, e) shows similar trend against different RHs. At a RH of ~45% in Figure 2(c), the log(τ) is around ~2, that is a τ of around several hundred seconds. This is equivalent to the time required from RH step changes, indicating the free transport of water within the particle bulk phase. When

RH is around ~35%, τ is around 2 orders of magnitude larger than τ at higher RH (> 60%), presenting strong effect from glassy state formation onto bulk phase water transfer and particle responses toward surrounding RH condition. Between the RH of ~0 - ~80%, τ changes for around 3 orders of magnitude. According to previous study,[41] the particle bulk phase viscosity exponentially increases with decreasing RH and increasing solute concentration, while D_{water} becomes smaller and bulk phase water transport is slower. This is consistent with phenomenon in our measurement. When the RH change across 35%, the inhibition of water transport is obvious (presented by huge increase of the particle size relaxation time). This illustrates strong kinetic inhibition on water transfer to the hygroscopic particle growth.

In Figure 2(b, d, f), stretched exponential behavior can be observed in all the size relaxation steps, including those steps corresponding to RHs smaller than the glass transition RH. The value of β correspond to RH increasing steps is larger than which correspond to RH decreasing steps. Under decreasing RH, water on the particle surface first evaporate, lead to formation of non-crystalline state layer. This thin layer thus inhibits the water transport from the interior of the particle, made the hygroscopic response of particle emerge into an relatively slow process. This is consistent with the trend of KWW curve with smaller β. Under increasing RH, water would condenses on the surface of the particle in the first several hundred seconds after RH is changed over multiple experimental stages.[5] During this period the condensed water form an infinite thin layer on the particle but has not been absorbed yet. This leads to a β larger than 1, [47] as larger β corresponds to longer induction time, while in a solely gas-diffusion limited condensation, there is no relationship between the size response and particle bulk composition.[48,49]

RH dependent D_{water} of sucrose/glucose aqueous particle is acquired from fittings of experimental results using the method from previous studies.[41,50] D_{water} represents the ability of water molecules transport in glassy aqueous particles. RH-D_{water} relationship with sucrose-glucose mass ratios of 3:1, 1:1,

and 1:3 are respectively illustrated with purple, dark cyan, and blue lines in Figure 3. All fittings and simulations in this study are conducted with the assumption that the levitated particle is an approximate sphere composed of concentric layers and the initial composition of particle bulk phase is homogeneous.[41] Thus, the infinite thin layer between the particle and surrounding gas phase is assumed to immediately reach gas-particle equilibrium after the RH is changed. The ZSR ideal mixing rule is also adopted in the calculations and simulations. As the formed non-crystalline state under lower RH is amorphous and would definitely influence light scattering within the particle, the measured result is more reliable at higher RH and with smaller corresponding RH step, as the value and changes of solute composition is smaller.

The RH-D_{water} of sucrose/glucose aqueous particle with different sucrose-glucose mass ratios show similar trend with results of sucrose aqueous particle from published studies as illustrated in Figure 3.[6,7,41] D_{water} at the highest RH limit is several orders larger than which at the lowest RH limit. This can be attributed to huge difference between the sizes of sugar molecule and water molecule. The fractional change in size is much lower in glassy particle, meaning the same length of experiment at lower RH will present a much worse signal to noise ratio. Therefore, the error envelope of D_{water} prediction at lower RH is larger.[51]

In order to contribute to better illustration of water transfer inhibition and its effect to the particle, we derive the evolving compositional in-homogeneities in the particle for evaporation and condensation steps, using the RH-D_{water} dependence shown in Figure 3, as the particle inhomogeneity would further influence important cloud physics properties. The time dependent water content at different radial coordinates the particle towards varying RH conditions are illustrated in Figure 4. Water distribution of particle in Figure 4(a, c, e) and (b, d, f) correspond to a ~30 to 5% RH decrease and an RH increase from ~5 to 30% for sucrose/glucose aqueous particle with 3 sucrose-glucose mass ratio, respectively. Both

water evaporation and condensation of non-crystalline particles are extremely slow. The deepest radial coordinates with observable responding water transport in Figure 4 is shown in Table 1. It is obvious that at 10000 s after the RH is changed, the particle is still quite far from reaching equilibrium with the surrounding conditions. Influence from water transfer inhibition is relatively higher for evaporation than condensation. Composition on the gas particle interface would respond rapidly towards surrounding RH changes. When the particle is dried to low RH, a sudden water evaporation through gas-particle interface would lead to a sudden and substantial limitation on diffusion by forming a crust on the particle's surface, prohibiting water transfer.[42] Conversely, when the particle experiences an increase in RH and corresponding water condensation, an aqueous solution shell is formed almost instantly and keeps equilibrium with the ambient gas phase, thus gradually dissolving the viscous interior part of particle. It is shown in Figure 4 that for both evaporation and condensation process, there are steep compositional gradients within the particle. The particle's hygroscopic response to changing RH environments would be most kinetically limited when the concentration gradient within the particle is the shallowest. Kinetic inhibitions would preclude accurate thermodynamics measurements as the particle is usually far from its equilibrium state under changed RH.

3.2. Water transport kinetics of $MgSO_4$ aqueous (gel state) particle

In the study of gel state particle, we present time dependent radius in a typical dehydration experimental data set. Figure 5 presents time dependent RH and corresponding radius of $MgSO_4$ aqueous particle. The water transfer inhibition in gel state particle is much more serious than which in glassy state particle, as there is little size relaxation response towards changing RH when RH is smaller than 40%. The characteristic equilibration time τ and β values of $MgSO_4$ aqueous particles are acquired using a

KWW fit and shown in Figure 6. The results was qualitatively consistent with trends in previous EDB studies of larger $MgSO_4$ particles,[48,49] presenting significant rise of τ under certain RH. At the dilute solute limit with high RH, τ is smaller than 10 min, indicating fast hygroscopic water transport through the gas-particle interface. When RH decreases, τ increased significantly as the particle first evolve to the ultra-viscous liquid and finally to the gel state, exhibiting bulk phase water transfer and indirectly retard particle size relaxation to the changing RH. Different from the observation of glassy sugar aqueous particle, the trends of τ and β towards different RHs is not that distinct. τ in condensation is relatively smaller than τ in evaporation, as water evaporation from viscous particle is slower than the dissolution of interior part of viscous particle.[5]

The RH-D_{water} relationship observed in gel state $MgSO_4$ aqueous particles is predicted with the exact method adopted for sugar ternary particle [41,50] and illustrated in Figure 7. D_{water} of $MgSO_4$ particle ranges from ~2.0×10^{-9} to 5.4×10^{-18} m^2 s^{-1} within the whole RH range. Although the RH-D_{water} relationship in Figure 7 present similar trend to results from sucrose-glucose aqueous particles, RH-D_{water} results for individual experimental sets are quite diverse, thus leads to an extremely large uncertainty envelope of RH-D_{water} relationship. It is suggested in our previous work that there is no clear dependence between D_{water} of $MgSO_4$ particles and RH. This could be the potential reason of the large uncertainty envelope of the RH-D_{water} relationship.

We further present simulated time-dependent compositional in-homogeneities of the $MgSO_4$ particle corresponding to ~30-5% RH decrease and ~5-30% RH increase with similar method for results of sugar ternary particle in Figure 4. Results corresponding to RH decrease and increase are shown in Figure 8(a) and (b), respectively. The deepest radial coordinates with observed responding water transport in Figure 8 is shown in Table 1. As shown in Figure 8 and

Table 1, the $MgSO_4$ particle registered much sharper concentration gradient than sugar ternary particle.

There is no compositional response toward RH changes in the interior part of particle with radial coordinate deeper than 0.7 for both evaporation and condensation processes, indicating much more serious water transport inhibition than which in sugar ternary particle. The presence of contact ion structures might contribute to this strong inhibition of bulk phase water transfer. The structure of $MgSO_4$ across different hydration levels have been detailed investigated with X-ray diffraction in previous studies.[53,54] The spatial structure of hydrated Mg-$(SO_4)_n$ would vary towards different water content. Thus the $MgSO_4$ aqueous particle would experience a phase transition from the cluster, through 2D layers, to a 3D framework with a decreasing RH. The 2D structure is much less sensitive to ambient RH than the cluster. In the 3D framework, water can only transport through thin channels and pores. This can be the potential reason for extremely slow water transport and bulk phase in-homogeneity of $MgSO_4$ aqueous particles and can explain the huge error envelope of RH-D_{water} relationship.

4. Conclusions

In this work, we assessed the water transfer inhibition effect in single levitated non-crystal particles during both evaporation and condensation, and provided a detailed description of water transport kinetics of multi-component particles during both processes. We quantitatively calculated RH dependent D_{water} of both glassy and gel particles. The results show that formation of non-crystalline state strongly limits bulk phase water transfer, thus inhibit hygroscopic response on the gas-particle interface. D_{water} of aqueous sucrose/glucose particles with sucrose/glucose mass ratio of 1:1 is ~2.22×10^{-16} m^2 s^{-1} at RH of ~20%. On the other hand, RH-D_{water} of gel state $MgSO_4$ particles is quite diverse from the gradual decrease of RH-D_{water} of glassy sugar aqueous particle, which resulted in large deviation envelope of D_{water} results. Bulk phase water transport in the evaporation process continued over a long timescale after fast initial

water transport on the particle gas interface, while water transport in condensation process was relatively faster on the whole. We illustrate water content at different particle radial coordinates and show the required timescale for a non-crystalline particle to reach equilibrium with its surrounding environment. This study illustrates a direct indication of retarded water diffusion within such atmospheric particles and its influence on partitioning and equilibrium between particles and surrounding gas phases.

Acknowledgments

The authors sincerely appreciate financial supports from the National Natural Science Foundation of China (Grant No. 41590872) and China Postdoctoral Science Foundation (the 62th batch of General Program, Grant No. 2017M620505). Prof. Jonathan P. Reid from University of Bristol, UK is sincerely appreciated for constructive suggestions and great efforts on text improvement. The authors declare no competing financial interest.

References

[1] E. Mikhailov, S. Vlasenko, S. T. Martin, T. Koop and U. Pöschl, *Atmos. Chem. Phys.* **9** (2009), 9491-9522.
[2] J. P. Reid, A. K. Bertram, D. O. Topping, A. Laskin, S. T. Martin, M. D. Petters, F. D. Pope and G. Rovelli, *Nat. Commun.* **9** (2018), 956.
[3] P. G. Debenedetti and F. H. Stillinger, *Nature* **410** (2001), 259-267.
[4] B. J. Murray and A. K. Bertram, *Phys. Chem. Chem. Phys.* **8** (2008), 5423-5433.
[5] D. L. Bones, J. P. Reid, D. M. Lienhard and U. K. Krieger, *Proc. Natl. Acad. Sci. USA* **109** (2012), 11613-11618.
[6] B. Zobrist, V. Soonsin, B. P. Luo, U. K. Krieger, C. Marcolli, T. Peter and T. Koop, *Phys. Chem. Chem. Phys.* **13** (2011), 3514-3526.
[7] B. Zobrist, C. Marcolli, D. A. Pedernera and T. Koop, *Atmos. Chem. Phys.* **8** (2008), 5221-5244.
[8] D. M. Lienhard, A. J. Huisman, D. L. Bones, Y. F. Te, B. P. Luo, U. K. Krieger and J. P. Reid, *Phys. Chem. Chem. Phys.* **16** (2014), 16677-16683.
[9] B. J. Murray, T. W. Wilson, S. Dobbie, Z. Q. Cui, S. M. R. K. Al-Jumur, M. Schnaiter, R. Wagner, S. Benz, M. Niemand, H. Saathoff, V. Ebert, S. Wagner and B. Karcher, *Nat. Geosci.* **3** (2010), 233-237.
[10] F. Wang, Y. Zhang, S. Li, L. Wang and L. Zhao, *Anal. Chem.* **77** (2005), 7148-7155.
[11] H. C. Price, J. Mattsson, Y. Zhang, A. K. Bertram, J. F. Davies, J. W. Grayson, S. T. Martin, D. O'Sullivan, J. P. Reid, A. M. J. Rickards and B. J. Murray, *Chem. Sci.* **6** (2015), 4876-4883.
[12] R. Saleh and A. Shihadeh, *Atmos. Meas. Tech.* **4** (2011), 571-581.

[13] D. M. Lienhard, A. J. Huisman, U. K. Krieger, Y. Rudich, C. Marcolli, B. P. Luo, D. L. Bones, J. P. Reid, A. T. Lambe, M. R. Canagaratna, P. Davidovits, T. B. Onasch, D. R. Worsnop, S. S. Steimer, T. Koop and T. Peter, *Atmos. Chem. Phys.* **15** (2015), 13599-13613.
[14] E. Abramson, D. Imre, J. Beránek, J. Wilson and A. Zelenyuk, *Phys. Chem. Chem. Phys.* **15** (2013), 2983-2991.
[15] V. Perraud, E. A. Bruns, M. J. Ezell, S. N. Johnson, Y. Yu, M. L. Alexander, A. Zelenyuk, D. Imre, W. L. Chang, D. Dabdub, J. F. Pankow and B. J. Finlayson-Pitts, *Proc. Natl. Acad. Sci. USA* **109** (2012), 2836-2841.
[16] C. M. Roth, K. U. Goss and R. P. Schwarzenbach, *Environ. Sci. Technol.* **39** (2005), 6638-6643.
[17] C. Liu, S. Shi, C. Weschler, B. Zhao and Y. Zhang, *Aerosol. Sci. Tech.* **47** (2012), 125-136.
[18] D. A. Knopf, L. M. Anthony and A. K. Bertram, *J. Phys. Chem. A* **109** (2005), 5579-5589.
[19] C. Pfrang, M. Shiraiwa and U. Poschl, *Atmos. Chem. Phys.* **11** (2011), 7343-7354.
[20] M. Shiraiwa, C. Pfrang and U. Poschl, *Atmos. Chem. Phys.* **10** (2010), 3673-3691.
[21] M. Shiraiwa, C. Pfrang, T. Koop and U. P. Schl, *Atmos. Chem. Phys.* **12** (2012), 2777-2794.
[22] C. J. Roberts and P. G. Debenedetti, *J. Phys. Chem. B* **103** (1999), 7308-7318.
[23] A. Virtanen, J. Joutsensaari, T. Koop, J. Kannosto, P. Yli-Pirilä, J. Leskinen, J. M. Mäkelä, J. K. Holopainen, U. Pöschl, M. Kulmala, D. R. Worsnop and A. Laaksonen, *Nature* **467** (2010), 824-827.
[24] L. Renbaum-Wolff, J. W. Grayson, A. P. Bateman, M. Kuwata, M. Sellier, B. J. Murray, J. E. Shilling, S. T. Martin and A. K. Bertram, *Proc. Natl. Acad. Sci. USA* **110** (2013), 8014-8019.
[25] D. Champion, H. Hervet, G. Blond, M. Le Meste and D. Simatos, *J. Phys. Chem. B* **101** (1997), 10674-10679.
[26] R. M. Power, S. H. Simpson, J. P. Reid and A. J. Hudson, *Chem. Sci.* **4** (2013), 2597-2604.
[27] M. Rampp, C. Buttersack and H. D. Ludemann, *Carbohydr. Res.* **328** (2000), 561-572.
[28] C. K. Chan, R. C. Flagan and J. H. Seinfeld, *J. Am. Ceram. Soc.* **81** (1998), 646-648.
[29] M. Mitterböck, G. Fleissner, A. Hallbrucker and E. Mayer, *J. Phys. Chem. B* **103** (1999), 8016-8025.
[30] B. J. Murray, A. E. Haddrell, S. Peppe, J. F. Davies, J. P. Reid, D. O'Sullivan, H. C. Price, R. Kumar, R. W. Saunders, J. M. C. Plane, N. S. Umo and T. W. Wilson, *Atmos. Chem. Phys.* **12** (2012), 8575-8587.
[31] S. Sjogren, M. Gysel, E. Weingartner, U. Baltensperger, M. J. Cubison, H. Coe, A. A. Zardini, C. Marcolli, U. K. Krieger and T. Peter, *J. Aerosol Sci.* **38** (2007), 157-171.
[32] A. A. Zardini, S. Sjogren, C. Marcolli, U. K. Krieger, M. Gysel, E. Weingartner, U. Baltensperger and T. Peter, *Atmos. Chem. Phys.* **8** (2008), 5589-5601.
[33] I. A. Farhat, E. Loisel, P. Saez, W. Derbyshire and J. M. V. Blanshard, *Int. J. Food Sci. Tech.* **32** (1997), 377-387.
[34] G. He, R. B. Tan, P. J. Kenis and C. F. Zukoski, *J. Phys. Chem. B* **111** (2007), 14121-14129.
[35] X. He, A. Fowler and M. Toner, *J Appl. Phys.* **100** (2006), 074702-11.
[36] R. J. Charlson, D. S. Covert, T. V. Larson and A. P. Waggoner, *Atmos. Environ.* **12** (1978), 39-53.
[37] L. Wang, F. Ding, Y. Zhang, L. Zhao and Y. Hu, *Spectrochim. Acta A* **71** (2008), 682-687.
[38] R. Buchner, T. Chen and G. Hefter, *J. Phys. Chem. B* **108** (2004), 2365-2375.
[39] K. Li, F. Wang, G. Zeng, J. P. Reid and Y. Zhang, *J. Phys. Chem. B* **115** (2011), 14397-14403.
[40] C. Cai and C. Zhao, *Atmos. Environ.* **189** (2018), 50-60.
[41] S. Ingram, C. Cai, Y. C. Song, D. R. Glowacki, D. O. Topping, S. O'Meara and J. P. Reid, *Phys. Chem. Chem. Phys.* **19** (2017), 31634-31646.
[42] A. M. Rickards, Y. C. Song, R. E. Miles, T. C. Preston and J. P. Reid, *Phys. Chem. Chem. Phys.* **17** (2015), 10059-10073.
[43] G. Williams and D. C. Watts, *Trans. Faraday Soc.* **66** (1970), 80-85.
[44] S. Sengupta, S. Karmakar, C. Dasgupta and S. Sastry, *J. Chem. Phys.* **138** (2013), 12A548.

[45] J. C. Phillips, *ReProg. Phys.* **59** (1996), 1133-1207.
[46] A. Amir, Y. Oreg and Y. Imry, *Proc. Natl. Acad. Sci. U. S. A.* **109** (2012), 1850-1855.
[47] R. A. Zaveri, R. C. Easter, J. E. Shilling and J. H. Seinfeld, *Atmos. Chem. Phys.* **14** (2014), 5153-5181.
[48] J. F. Davies, A. E. Haddrell, R. E. H. Miles, C. R. Bull and J. P. Reid, *J. Phys. Chem. A* **116** (2012), 10987-10998.
[49] J. F. Davies, A. E. Haddrell and J. P. Reid, *Aerosol. Sci. Tech.* **46** (2012), 666-677.
[50] S. O'Meara, D. O. Topping and G. Mcfiggans, *Atmos. Chem. Phys.* **16** (2016), 1-25.
[51] Y. Zhang, C. Cai, S. F. Pang, J. P. Reid and Y. H. Zhang, *Phys. Chem. Chem. Phys.* **19** (2017), 29177-29186.
[52] C. Cai, S. H. Tan, H. N. Chen, J. B. Ma, Y. Wang, J. P. Reid and Y. H. Zhang, *Phys. Chem. Chem. Phys.* **17** (2015), 29753-29763.
[53] H. Ma, D. L. Bish, H. W. Wang and S. J. Chipera, *Am. Mineral.* **94** (2009), 622-625.
[54] H. Ma, D. L. Bish, H. W. Wang and S. J. Chipera, *Am. Mineral.* **94** (2009), 1071-1074.

Table 1. The deepest radial coordinates with observable responding water transport in Figure 4 and Figure 8.

RH decreasing		**Particle solute composition**			
Completed water transport fraction		**mf(Sucrose): mf(Glucose) = 3:1**	**mf(Sucrose): mf(Glucose) = 1:1**	**mf(Sucrose): mf(Glucose) = 1:3**	**$MgSO_4$**
Timing after RH is changed / s	**10**	0.979	0.978	0.975	0.980
	30	0.977	0.974	0.969	0.980
	100	0.971	0.965	0.953	0.979
	300	0.959	0.947	0.922	0.977
	1 000	0.931	0.904	0.845	0.970
	3 000	0.873	0.812	0.686	0.957
	10 000	0.727	0.604	0.384	0.928
RH increasing		**Particle solute composition**			
Completed water transport fraction		**mf(Sucrose): mf(Glucose) = 3:1**	**mf(Sucrose): mf(Glucose) = 1:1**	**mf(Sucrose): mf(Glucose) = 1:3**	**$MgSO_4$**
Timing after RH is changed / s	**10**	0.976	0.973	0.967	0.980
	30	0.969	0.963	0.951	0.980
	100	0.953	0.941	0.918	0.978
	300	0.925	0.903	0.861	0.975
	1 000	0.868	0.824	0.740	0.966
	3 000	0.767	0.681	0.491	0.950
	10 000	0.528	0.264	0.010	0.917

394 **Figure 1.** Time dependent RH from probe (a, red) and particle radius (b, blue) of a levitated
395 sucrose/glucose aqueous particle in a typical experiment.

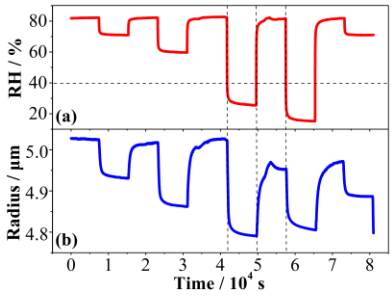

396

Figure 2. Exponential folding time, τ, of particle radius responses of sucrose/glucose aqueous particles with sucrose-glucose mass ratio of (a) mf(sucrose):mf(glucose) = 3:1, (c) mf(sucrose):mf(glucose) = 1:1, and (e) mf(sucrose):mf(glucose) = 1:3 to RH steps mapped over initial and final values, with corresponding stretched exponential parameter, β, extracted for the same transitions by allowing it to vary during the fitting process.

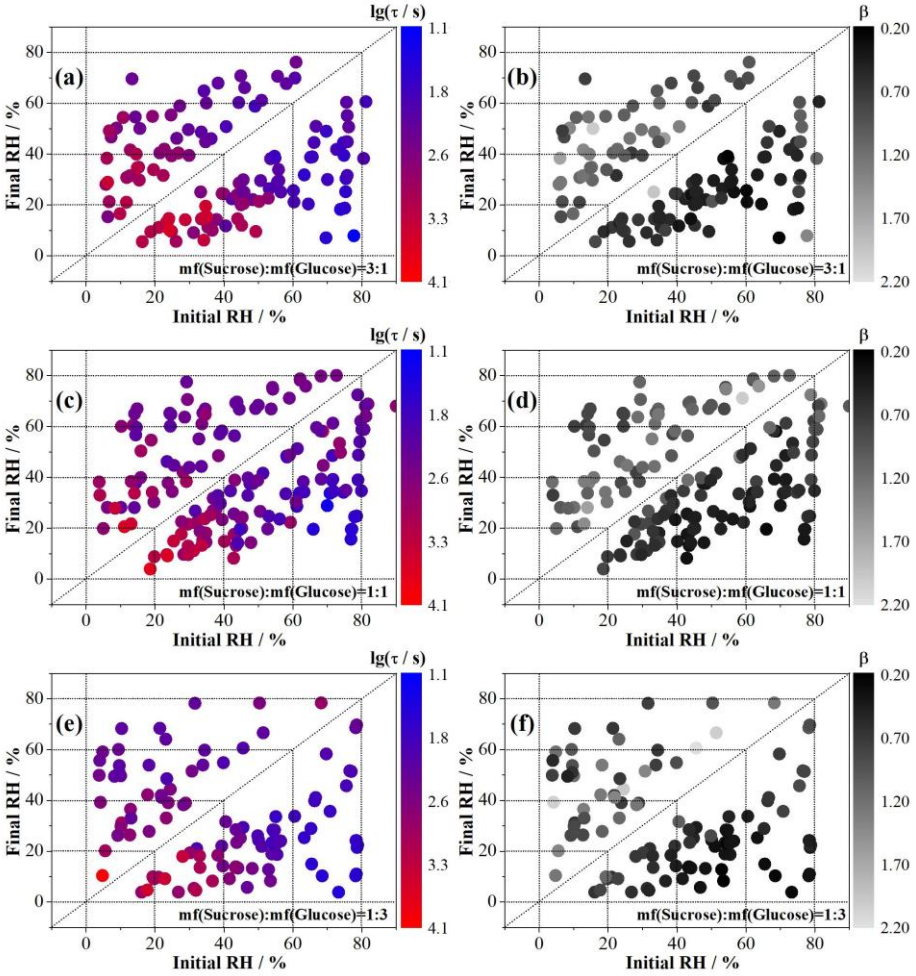

Figure 3. Composition dependent D_{water} estimated from RH transitions in sucrose/glucose aqueous particles with sucrose-glucose mass ratio of 3:1 (purple), 1:1 (dark cyan), and 1:3 (blue).

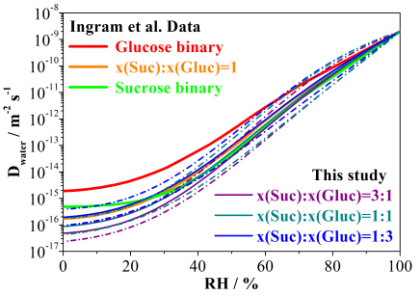

Figure 4. Simulations of heterogeneity in levitated sucrose/glucose aqueous particle with sucrose-glucose mass ratio of 3:1 (a, b),1:1 (c, d) and 1:3 (e, f) during dehumidifying (a, c, e) and humidifying (b, d, f) processes between 30% and 5% RH. The initial particle radius is 3500 nm. The thermodynamic treatment and diffusion coefficient parameterization from reported studies[41,50] is used. Lines with different colors represent times after the RH change of 0 s (red), 10 s (orange), 30 s (yellow), 100 s (grass), 300 s (green), 1000 s (spring green), 3000 (cyan), and 10000 s (blue).

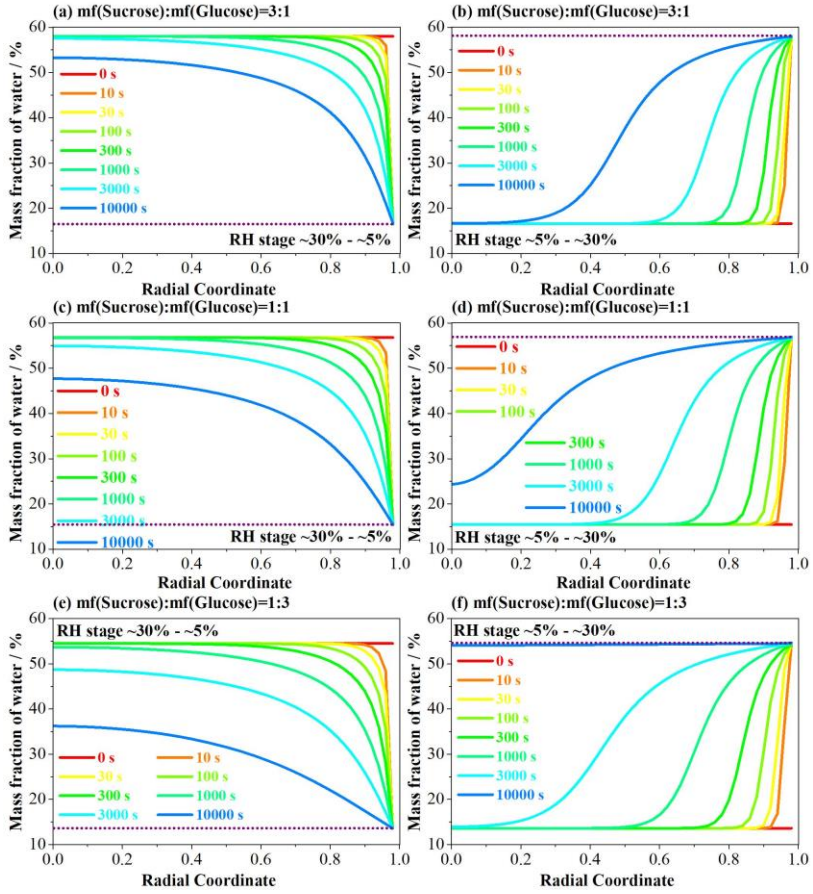

Figure 5. Time dependent RH from probe (a, red) and radius (b, blue) of a levitated $MgSO_4$ aqueous particle in a typical measurement.

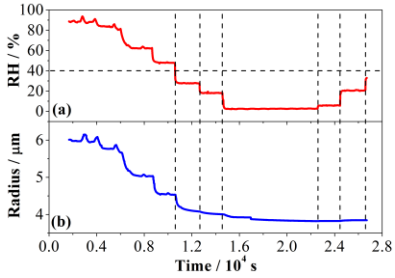

Figure 6. (a) Exponential folding time, τ, for changes in the size of an $MgSO_4$ aqueous particle from optical tweezers measurements (solid circles) mapped with different mapped colors; (b) Corresponding stretched exponential parameter, β, extracted for the same transitions by allowing it to vary during the fitting process. The shaded area identifies the RH region where the particle exists as a gel.

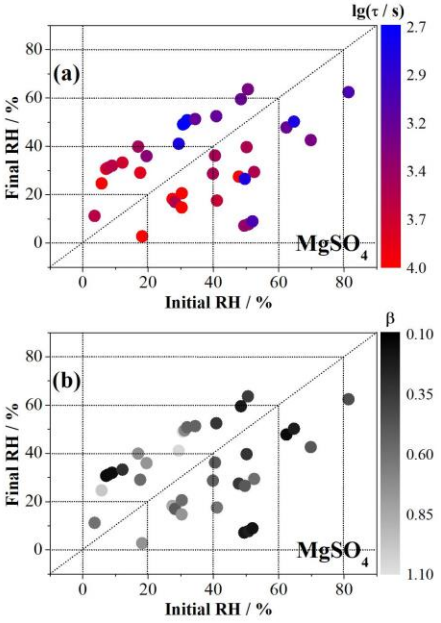

421 **Figure 7.** D_{water} estimated from RH transitions in $MgSO_4$ aqueous particles to RH steps.

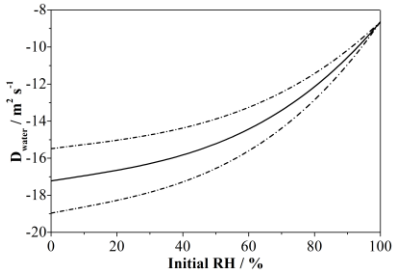

422

Figure 8. Simulations of heterogeneity in levitated $MgSO_4$ aqueous particle during dehumidifying (a) and humidifying (b) processes between 30% and 5% RH. The initial particle radius is 3500 nm. The thermodynamic treatment and diffusion coefficient parameterization from reported studies [41,50] is used. Lines with different colors represent times after the RH change of 0 s (red), 10 s (orange), 30 s (yellow), 100 s (grass), 300 s (green), 1000 s (spring green), 3000 (cyan), and 10000 s (steel blue).